

Advanced Dynamics of Mechanical Systems
Assignment 1

Tommaso Bocchietti 10740309

A.Y. 2023/24



POLITECNICO
MILANO 1863

Contents

| | |
|--|-----------|
| 1 Requests (Part A) | 3 |
| 2 Computation of natural frequencies and mode shapes | 3 |
| 2.1 Computation of natural frequencies | 4 |
| 2.2 Computation of mode shapes | 4 |
| 3 Computation of FRFs | 5 |
| 3.1 FRFs of the system due to a single point force | 6 |
| 3.2 FRFs of the system due to a multiple point force | 7 |
| 4 Parameters identification | 8 |
| 4.1 Procedure | 9 |
| 4.2 Parameters identification results | 10 |
| 5 Final results (mode shapes comparison) | 11 |
| 6 Requests (Part B) | 13 |
| 7 Data Analysis | 13 |
| 7.1 First peak | 13 |
| 7.2 Second peak | 13 |
| 8 Final Results (mode shapes visualization) | 14 |

List of Figures

| | |
|--|----|
| 1 Aluminum beam with rectangular cross-section | 3 |
| 2 Numerical search for natural frequencies of the system. Minimums value of $\det[H(\omega)]$ are considered as natural frequencies. | 4 |
| 3 Computed mode shapes starting from the ideal model of the cantilever beam. | 5 |
| 4 Analyzed situation: single input, multiple outputs | 6 |
| 5 FRFs of the system due to a single point force. Each color in the plot represents the FRF of the structure at a specific output coordinate. | 7 |
| 6 Analyzed situation: multiple inputs, multiple outputs | 7 |
| 7 Complex plane representation of the FRFs of the system due to multiple input forces and the actual displacement of the output/interrogation point. | 8 |
| 8 FRFs of the system due to a couple of point force. Each color in the plot represents the FRF of the structure at a specific output coordinate. | 8 |
| 9 FRF identification for $x_k = 1.0m$ and $y_j = 0.6m$ | 10 |
| 10 Zoom over the peaks of the FRF identification for $x_k = 1.0m$ and $y_j = 0.6m$ | 11 |
| 11 Comparison between experimental and numerical mode shapes | 12 |
| 12 FRFs and coherence functions of the system. | 13 |
| 13 First peak FRFs comparison. | 14 |
| 14 Second peak FRFs comparison. | 14 |
| 15 Identified (numerically) first two mode shapes of the system. | 14 |
| 16 First mode shape of the system visualized in a 3D way. Credit to [1]. | 15 |

List of Tables

| | |
|---|----|
| 1 Parameters of the cantilever beam | 3 |
| 2 Entities explanation for Equation 9 | 6 |
| 3 Relative error between experimental (in this case coming the flexible body theory) and numerical natural frequencies. | 12 |
| 4 First peak modal parameters. | 13 |
| 5 Second peak modal parameters. | 14 |
| 6 Identified parameters for the first two mode shapes of the system. | 15 |

1 Requests (Part A)

The requests for ‘Assignment 1 (Part A)’ are the followings:

- Briefly describe the procedure followed for computing natural frequencies and mode shapes. Plot the mode shapes of the first four modes with the indication of the associated natural frequencies and provide comments to the results.
- Compute the FRFs for some combinations of input and output positions. Comment the results.
- Briefly describe the procedure followed for identifying the natural frequencies, damping ratios and mode shapes of the first four modes, relying on the FRF-based multi-mode curve fitting method ($n = 1$).
- Check the quality of the identification comparing the identified FRFs and the ones numerically computed.
- Compare the parameters defined at the simulation stage to the identified ones. Collect the results in table form and plot a diagram showing the comparison of the simulated and identified mode shapes.

2 Computation of natural frequencies and mode shapes

For the problem at hand, we are dealing with a cantilever beam (see Figure 1) with parameters as shown in Table 1.

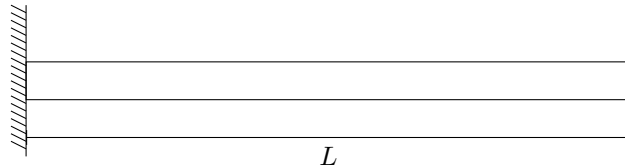


Figure 1: Aluminum beam with rectangular cross-section

| Parameter | Symbol | Unit | Value |
|-----------------|--------|-------------------|-------|
| Length | L | mm | 1200 |
| Thickness | h | mm | 8 |
| Width | b | mm | 40 |
| Density | ρ | kg/m ³ | 2700 |
| Young's modulus | E | GPa | 68 |

Table 1: Parameters of the cantilever beam

For this type of system/structure, considering zero axial-load, the standing wave equation governing its dynamics is:

$$EJ \frac{\partial^4 u}{\partial x^4} = -\rho A \frac{\partial^2 u}{\partial t^2} \quad (1)$$

Which, when fully solved, leads to the following formulation of vertical displacement over time $w(x, t)$:

$$w(x, t) = [A \cos(\gamma x) + B \sin(\gamma x) + C \cosh(\gamma x) + D \sinh(\gamma x)] \cos(\omega t + \phi) \quad (2)$$

Where $\gamma^4 = \frac{m\omega^2}{EJ}$.

By applying the boundary conditions of the cantilever beam, we can find the natural frequencies (and successively also the mode shapes) of the system. The equations that must be satisfied are:

$$\begin{cases} w(0, t) = 0 \\ \frac{\partial w}{\partial x}(0, t) = 0 \\ \frac{\partial^2 w}{\partial x^2}(L, t) = 0 \\ \frac{\partial^3 w}{\partial x^3}(L, t) = 0 \end{cases} \quad (3)$$

By highlighting the four unknowns A , B , C and D , and rearranging the equations in a matrix form, we end up with a linear system as:

$$[H(\omega)]z = \begin{bmatrix} 1 & 0 & 1 & 0 \\ 0 & 1 & 0 & 1 \\ -\cos(\gamma L) & -\sin(\gamma L) & +\cosh(\gamma L) & +\sinh(\gamma L) \\ +\sin(\gamma L) & -\cos(\gamma L) & +\sinh(\gamma L) & +\cosh(\gamma L) \end{bmatrix} \begin{bmatrix} A \\ B \\ C \\ D \end{bmatrix} = \begin{bmatrix} 0 \\ 0 \\ 0 \\ 0 \end{bmatrix} \quad (4)$$

2.1 Computation of natural frequencies

From theory, we know that the natural frequencies of a system can be computed by solving the following equation:

$$\det[H(\omega_n)] = 0 \quad (5)$$

Where $H(\omega_n)$ is the matrix as reported in Equation 4 and ω_n is one of the natural frequencies.

By iterating over a given vector of frequencies, we can compute the value of the determinant of the matrix $H(\omega)$ and find the minimums, which correspond to the natural frequencies of the system.

The result of this computation is shown in Figure 2.

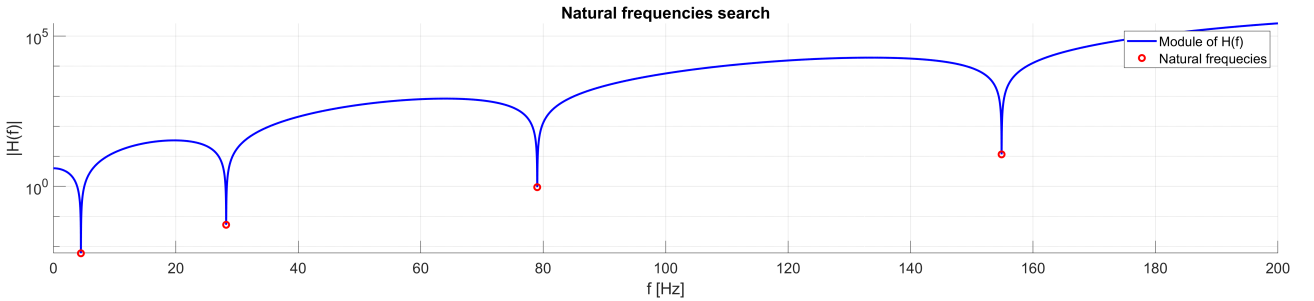


Figure 2: Numerical search for natural frequencies of the system. Minimum values of $\det[H(\omega)]$ are considered as natural frequencies.

2.2 Computation of mode shapes

The mode shapes of the system can be computed again by considering the system of Equations 4.

In particular, given that to each natural frequency ω_n corresponds a mode shape, we can compute the mode shapes by solving the linear system for each natural frequency. However, even if the system is exactly the same, it's important to understand that our goal now is to find the values of A , B , C and D that satisfy the system of equations, rather than finding the natural frequencies that cancel H .

In the end we will have a set of mode shapes, each one corresponding to a natural frequency of the system:

$$H(\omega_{n,i})z_i = 0 \quad (6)$$

By imposing the first component of the solution vector z_i to be $A = 1$, we can find the other components of the solution vector.

$$[H(\omega_{n,i})]z_i \rightarrow \hat{z}_i = \begin{bmatrix} B \\ C \\ D \end{bmatrix} = - \begin{bmatrix} 1 & 0 & 1 \\ -\sin(\gamma L) & +\cosh(\gamma L) & +\sinh(\gamma L) \\ -\cos(\gamma L) & +\sinh(\gamma L) & +\cosh(\gamma L) \end{bmatrix}^{-1} \begin{bmatrix} 0 \\ -\cos(\gamma L) \\ +\sin(\gamma L) \end{bmatrix} \quad (7)$$

Once all the mode shapes coefficients ($A = 1$, B , C and D) are computed, we can plot them with the indication of the associated natural frequency (see Figure 3).

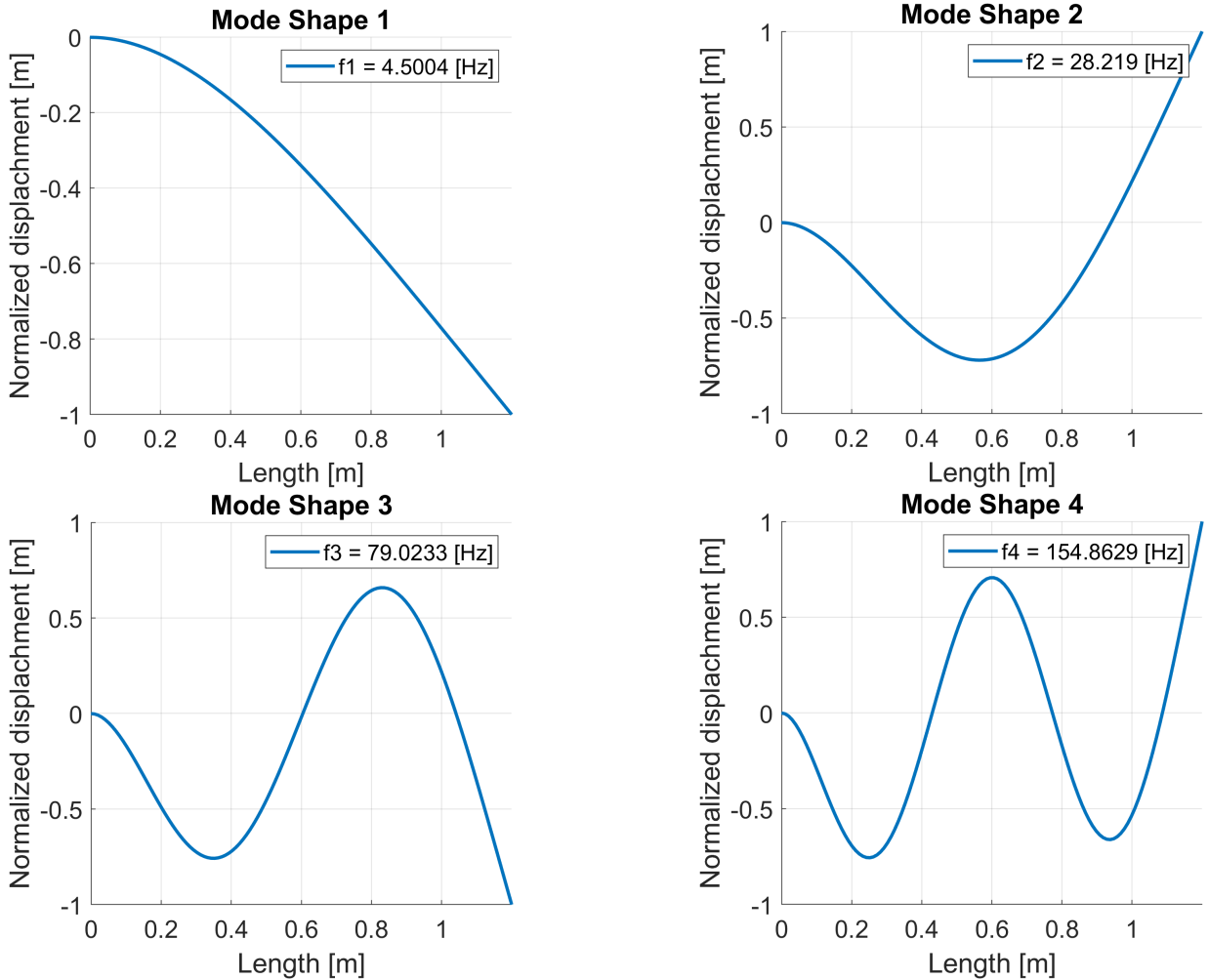


Figure 3: Computed mode shapes starting from the ideal model of the cantilever beam.

3 Computation of FRFs

The computation of the FRFs is a crucial step in the analysis of the dynamic behavior of a structure. The FRF is a complex-valued function that describes the steady-state response of a system to a sinusoidal excitation. Even if the restriction over the shape of the excitation is quite severe, the FRF is a powerful tool to analyze the dynamic behavior of a system given that due to the linearity of the system, the response to a general excitation can be obtained by a linear combination of the responses to sinusoidal excitations (Fourier series).

By definition, the FRF is the ratio of the output to the input in the frequency domain. For a linear time-invariant system, the FRF is a complex-valued function of the frequency, and it is defined as:

$$H(\omega) = \frac{Y(\omega)}{X(\omega)} \quad (8)$$

Where $H(\omega)$ is the FRF, $Y(\omega)$ is the Fourier transform of the output signal $y(t)$, and $X(\omega)$ is the Fourier transform of the input signal $x(t)$.

Moreover, to give a more practical definition, the FRF is the function that relates the output of a system considered at a specific coordinate to a sinusoidal input at a given coordinate. If we then consider the system to be linear, time-invariant, and with a single input $\Phi_i(x_k)$ and a single output $\Phi_i(x_j)$, than the FRF can be defined as:

$$H_{j,k}(\Omega) = \sum_{i=1}^n \frac{\Phi_i(x_j)\Phi_i(x_k)/m_i}{-\Omega^2 + 2\xi_i\omega_i\Omega i + \omega_i^2} \quad (9)$$

Where, all the entities of Equation 9 are defined in Table 2.

| Parameter | Description |
|---------------|---|
| $\Phi_i(x^*)$ | Mode shape of the i^{th} mode at coordinate x^* |
| m_i | Equivalent mass of the i^{th} mode |
| ξ_i | Damping ratio of the i^{th} mode |
| ω_i | Natural frequency associated to the i^{th} mode |
| Ω | Frequency of the sinusoidal excitation |

Table 2: Entities explanation for Equation 9

As we can notice, among the entities of Equation 9, at the moment we are only missing the equivalent mass m_i and the damping ratio ξ_i .

The equivalent mass m_i is a fictitious value that represents the amount of mass of the system that is effectively moving in the i^{th} mode, weighted by the mode shape. From this definition, we get:

$$m_i = \int_0^L \rho A \Phi_i^2(x) dx \quad (10)$$

For the damping ratio ξ_i , we can either use the Rayleigh damping model or the modal damping model. However, since we are not dealing with a discretized system, but rather with a continuous one, for the sake of simplicity we will assume the damping ratio to be $\xi_i = \frac{c_i}{2\sqrt{m_i k_i}} = 0.01$.

By doing so, we can compute the FRFs for the system at hand, and we can analyze the dynamic behavior of the structure.

3.1 FRFs of the system due to a single point force

Once the FRFs function is defined, we can think of interrogate the structure to see how it reacts due to a single point force applied at a specific coordinate.

In particular, we can consider a sinusoidal force applied at coordinate $x_k = 0.9m$ and see how the structure reacts at a set of coordinates $x_j = [0.2 \ 0.4 \ 0.6 \ 0.8 \ 1.0 \ 1.2]m$. A graphical representation of the considered situation can be seen in Figure 4.

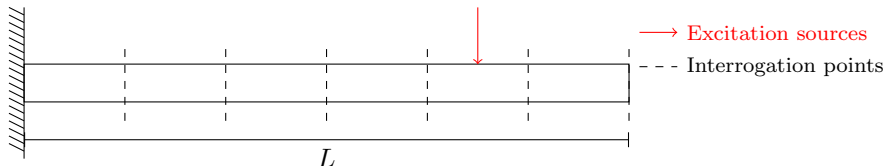


Figure 4: Analyzed situation: single input, multiple outputs

Since we are now considering 6 different coordinates, we will have 6 different FRFs, each one describing the response of the structure at a specific coordinate due to the excitation $f(t) = F_0 \sin(\Omega t) = 1 \sin(\Omega t)$.

By doing so, we obtain the module and phase plots reported in Figure 5.

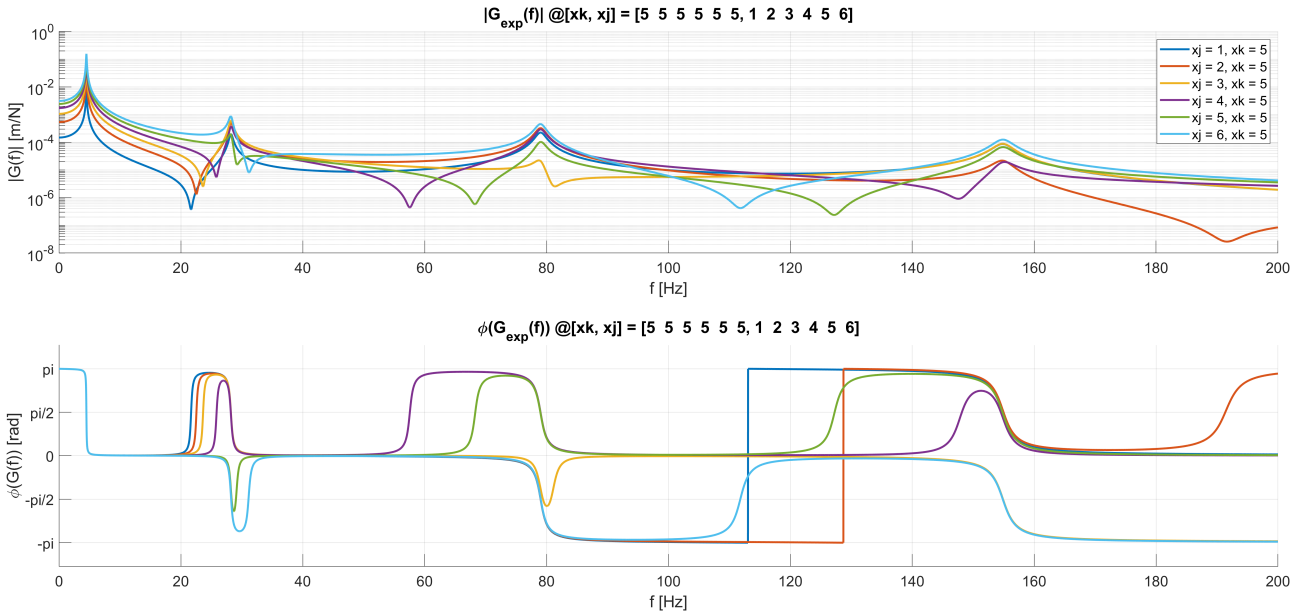


Figure 5: FRFs of the system due to a single point force. Each color in the plot represents the FRF of the structure at a specific output coordinate.

3.2 FRFs of the system due to a multiple point force

The next step is to observe the behavior of the structure when multiple forces are applied to it. As we have said in the previous section, even if the FRF given information about a single input and a single output, we can still use it to understand how the structure behaves when multiple forces are applied to it and study the structural response at different coordinates.

For the sake of simplicity, we will consider a structure with 2 excitation points at $x_k = [0.3 \ 0.9]\text{m}$ and 3 output points at $x_j = [0.2 \ 0.8 \ 1.2]\text{m}$.

A graphical representation of the considered situation can be seen in Figure 6.

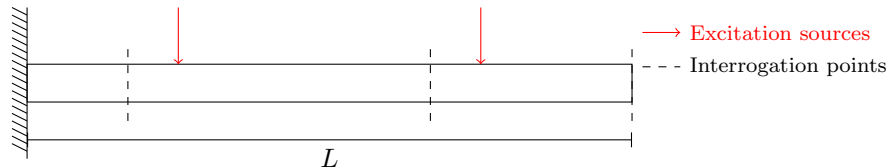


Figure 6: Analyzed situation: multiple inputs, multiple outputs

Similar reasoning as before can be done about the expected result of this type of analysis in terms of number of FRFs to be computed and the information that can be extracted from them.

Moreover, given that we are now dealing with a multi-input system, the actual displacement of the structure at a specific coordinate will be the result of the superposition of the displacements due to each excitation force. Before proceeding with the visualization of the actual FRFs, it's important to stress that what we are actually "superposing" are the complex FRFs, not only their modules. This means that the phase information is also taken into account when computing the total response of the structure (which indeed depends on the phase of the input forces).

To better understand this aspect, we can move on a complex plane and consider the output of a generic system due to two different input forces $F_1 = F_{1,0} \sin(\omega_1 t + \phi_1)$ and $F_2 = F_{2,0} \sin(\omega_2 t + \phi_2)$.

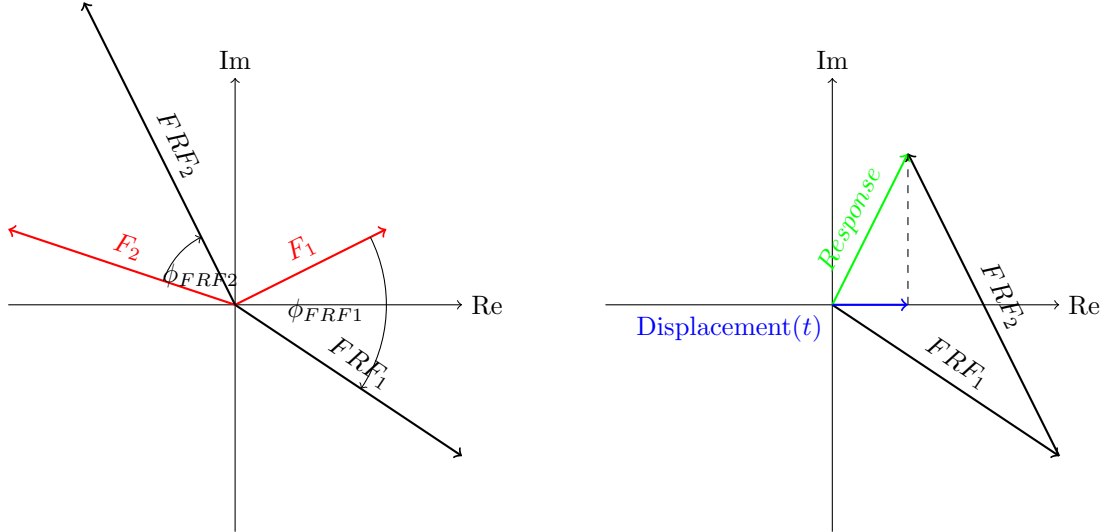


Figure 7: Complex plane representation of the FRFs of the system due to multiple input forces and the actual displacement of the output/interrogation point.

As is clearly seen in Figure 7, the actual displacement of the output point can in some cases (or better for some period of time) be definitely lower than the sum of just the absolute modules of the FRFs. Notice, however, that if the two acting forces have different periods (frequencies), there also be some time instants where the actual displacement is effectively the sum of the two modules of the FRFs. So in general, if we are just interested in the maximum displacement of the output point, we can simply sum the modules of all the FRFs due to the different input forces.

If we go back and considering again the situation represented in Figure 6, we obtain the module and phase plots reported in Figure 8.

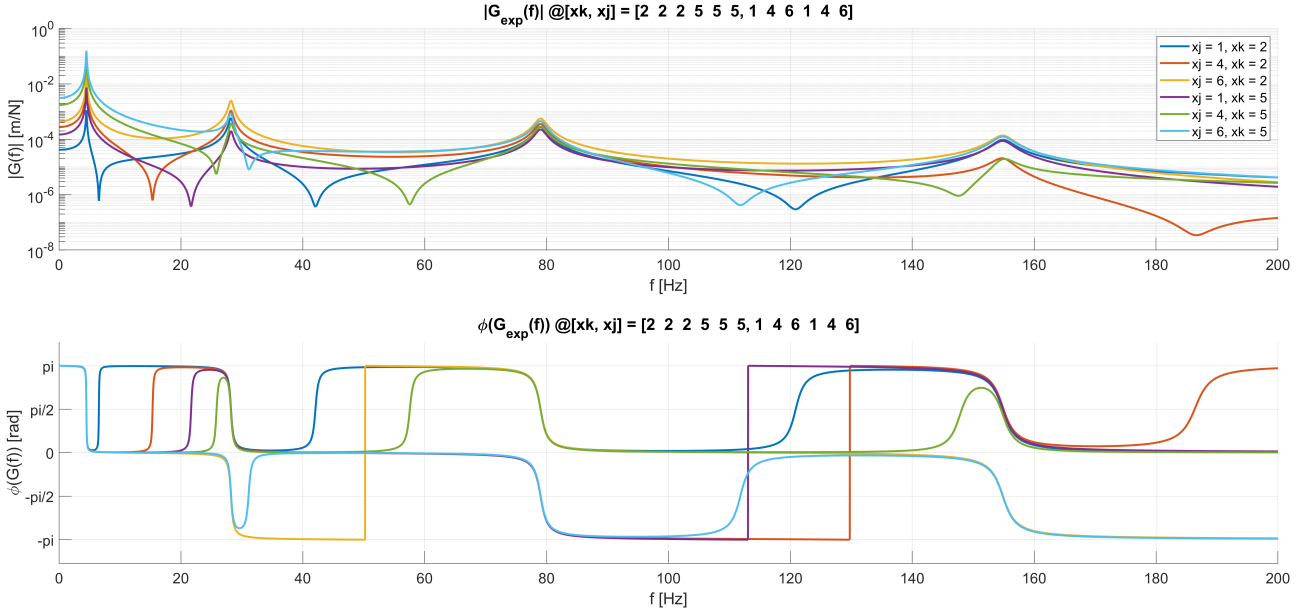


Figure 8: FRFs of the system due to a couple of point force. Each color in the plot represents the FRF of the structure at a specific output coordinate.

4 Parameters identification

In this section, we are going to explain the procedure followed to identify the parameters of the system starting from the FRFs obtained in the previous section. Basically we are going to simulate an ‘Operational Modal Analysis’ (OMA), even if in this case we already have the exact model of the system.

In particular, we know that for a multi degree-of-freedom system, with lightly damped modes and in particular in case of well distinguished peaks, the FRF can be approximated around a given natural frequency ω_n as:

$$H_{j,k}^{NUM}(\Omega) = \frac{A_{j,k}^{(i)}}{-\Omega^2 + 2\xi_i\omega_i\Omega + \omega_i^2} + \frac{R_{j,k}^L}{\Omega^2} + R_{j,k}^H \quad \text{for } \Omega_{min} \leq \omega_i \leq \Omega_{max} \quad (11)$$

As we can see, the FRF is approximated as a sum of three terms: a second order term, a low frequency term and a high frequency term. The second order term is the one that we are interested in, since it is the one that contains the information about the natural frequency and the damping ratio of the system. However, if the peaks are not well distinguished, the low and high frequency terms can interfere with the second order term and become non-negligible in the approximation.

In the following, a common procedure is explained to identify all the unknown parameters of $H_{j,k}^{NUM}(\Omega)$, once the experimental FRFs are available. In particular, we will see how to identify the natural frequencies ω_i^{NUM} , the damping ratios ξ_i^{NUM} , and the gains $A_{j,k}^{NUM}$, $R_{j,k}^L$ and $R_{j,k}^H$, using minimization techniques.

4.1 Procedure

Many of the following steps are based on the assumption that the frequencies vector defining the FRFs, has a higher enough resolution to properly address the following procedure. In case of a low resolution, the frequencies vector should be at least interpolated in order to obtain a more fine grid over the frequency range of interest. All the following steps, must be repeated for each natural frequency ω_i of the system.

Natural frequencies The first step is to identify the value of the natural frequency ω_i^{NUM} of the system. This can be done by looking at the peaks of the FRFs. If we have many FRFs at our disposal (for example, we have many sensors or we have performed many tests), we can average the FRFs in order to reduce the noise and obtain a more reliable result. Remember that the natural frequency identified has to be the same for all the FRFs.

Damping ratios The second step is to identify the value of the damping ratio ξ_i^{NUM} of the system. For this purpose, we can use both the ‘phase derivative’ method or the ‘half power bandwidth’ method (also known as ‘peak picking’ method).

For this assignment, we decided to use the ‘phase derivative’ method, given that the experimental FRFs have a fine enough grid of frequencies.

By looking at the phase of the FRF evaluated at the natural frequency ω_i , we observe that the slope of the phase can be directly related to the damping ratio ξ_i . In particular:

$$\left. \frac{\partial \angle H_{j,k}(\Omega)}{\partial \Omega} \right|_{\Omega=\omega_i} = -\frac{1}{\xi_i \omega_i} \quad (12)$$

Based on this relation, we can isolate the damping ratio ξ_i and obtain its value numerically, computing the derivative of the phase of the FRF evaluated at the natural frequency ω_i using a finite difference method.

$$\xi_i^{NUM} = -\frac{1}{\omega_i^{NUM} \cdot \frac{\Delta \angle G_{i,k}^{NUM}(\omega_i^{NUM})}{\Delta \omega}} \quad (13)$$

Gain $A_{j,k}^{NUM}$ The third step is to identify the value of the gain $A_{j,k}^{NUM}$ of the system.

This can be done by looking at the magnitude of the FRFs evaluated at the natural frequency ω_i . In particular, we can obtain the value of the gain $A_{j,k}^{NUM}$ numerically as:

$$A_{j,k}^{NUM} = -2i |G_{j,k}^{EXP}(\omega_i^{NUM})| \omega_i^2 \xi_i^{NUM} \quad (14)$$

However, in order to reduce the disturbances effects coming from the low and high frequency terms, we decided to use a more robust method to identify the gain $A_{j,k}^{NUM}$, relying on just the imaginary part of the FRF evaluated at the natural frequency ω_i :

$$A_{j,k}^{NUM} = -Im [2 |G_{j,k}^{EXP}(\omega_i^{NUM})| \omega_i^2 \xi_i^{NUM}] \quad (15)$$

Final minimization algorithm Finally, we can proceed with the minimization of the error between the experimental FRFs and the model FRFs, in order to identify the ‘exact’ values of all the parameters of the system, since the previous steps are only needed as a first approximation.

To do so, we define the error function as:

$$\epsilon = \sum_{j,k,\Omega} |H_{j,k}^{NUM}(\Omega) - H_{j,k}^{EXP}(\Omega)|^2 \quad (16)$$

Which we can think of as the sum of the squared differences between the experimental FRFs and the numerical FRFs evaluated at all the considered frequencies around the analyzed natural frequency ω_i . In order to minimize the error function, we can use a minimization algorithm, such as the ‘Levenberg-Marquardt’ algorithm, which is a combination of the ‘Gauss-Newton’ algorithm and the ‘Steepest Descent’ algorithm. This algorithm is particularly useful in case of non-linear least squares problems, such as the one we are facing. In MATLAB, the ‘Levenberg-Marquardt’ algorithm is implemented in the function `lsqnonlin`.

4.2 Parameters identification results

Once the previously explained procedure has been applied to all the natural frequencies of the system (consider for each one, every experimental FRFs at our disposal), we can reassemble the identified parameters so to compute the numerical FRFs of the system based on Equation 11.

In the following figures, the result obtained considering the FRF relative to an input in $x_k = 1.0m$ and an output in $y_j = 0.6m$ is shown.

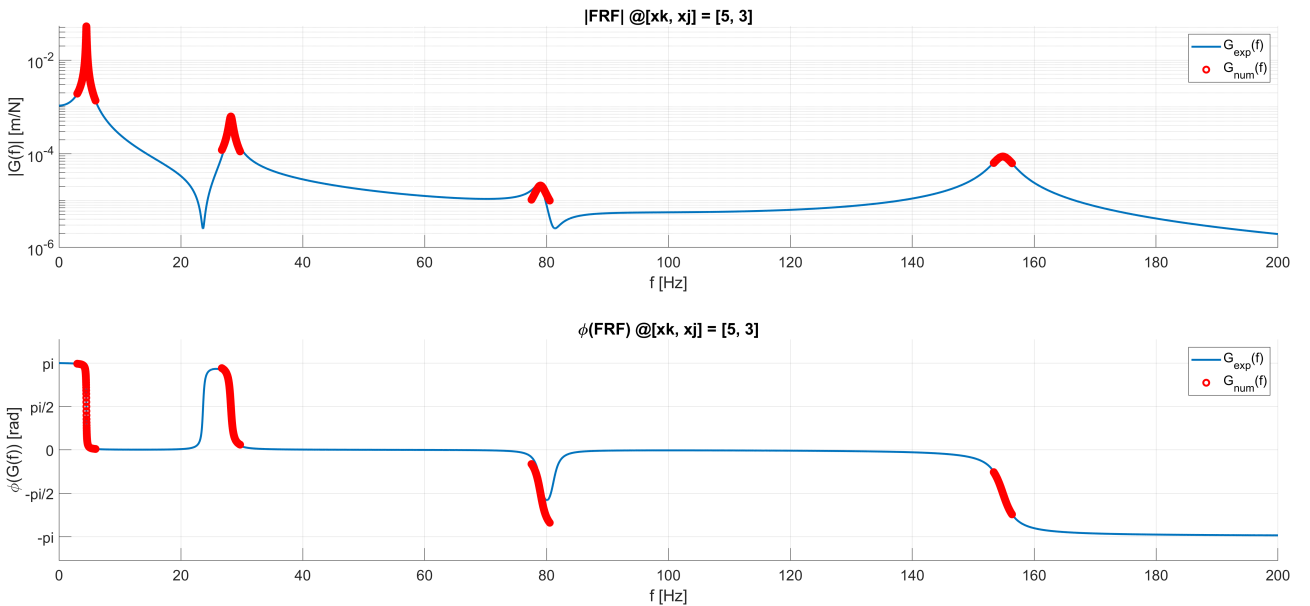


Figure 9: FRF identification for $x_k = 1.0m$ and $y_j = 0.6m$

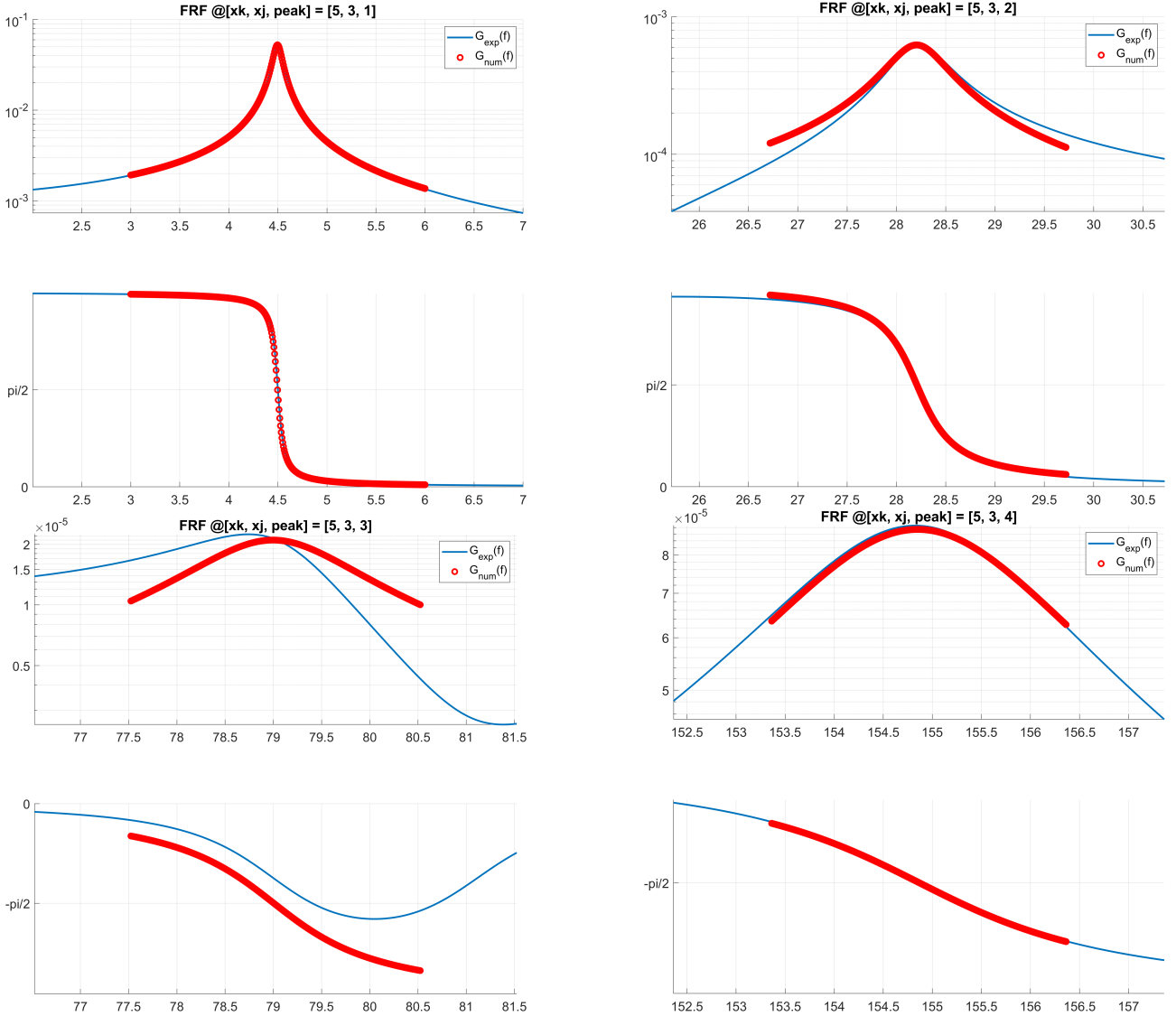


Figure 10: Zoom over the peaks of the FRF identification for $x_k = 1.0m$ and $y_j = 0.6m$

5 Final results (mode shapes comparison)

Even if the comparison between the experimental FRFs and the numerical FRFs in the complex plane is a good way to validate the identified parameters, it is also useful to compare the mode shapes obtained from the experimental data with the ones obtained from the numerical model.

In the following figures, the experimental (from flexible body theory) and numerical mode shapes are compared for the first 4 modes of the system.

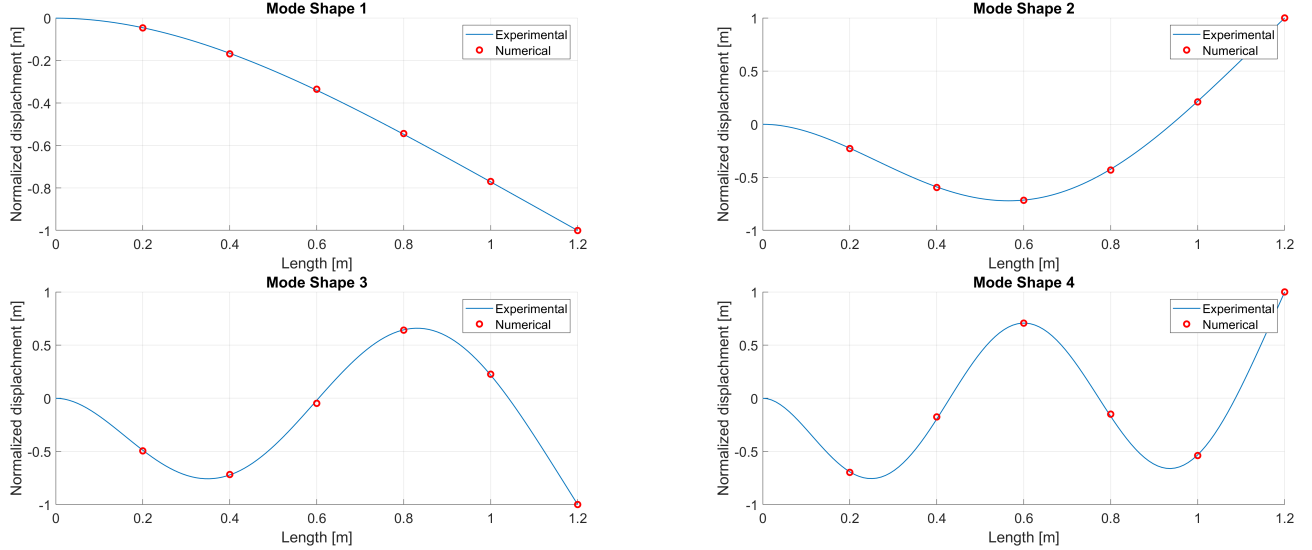


Figure 11: Comparison between experimental and numerical mode shapes

Numerically speaking, we can also report the relative error between the experimental and numerical natural frequencies, defined as follows:

$$\text{Relative error} = \frac{\sum_{i=1}^N |\omega_{\text{exp},i} - \omega_{\text{num},i}|}{\sum_{i=1}^N |\omega_{\text{exp},i}|} \% \quad (17)$$

Where $\omega_{\text{exp},i}$ and $\omega_{\text{num},i}$ are the i -th experimental and numerical natural frequencies, respectively. The relative error for the first 4 natural frequencies of the system is reported in the following table.

| Mode | Experimental [rad/s] | Numerical [rad/s] | Relative error [%] |
|------|----------------------|-------------------|--------------------|
| 1 | 28.2767 | 28.2524 | 0.0859 |
| 2 | 177.3053 | 177.2344 | 0.0400 |
| 3 | 496.5177 | 496.3996 | 0.0238 |
| 4 | 973.0323 | 973.0560 | -0.0024 |

Table 3: Relative error between experimental (in this case coming the flexible body theory) and numerical natural frequencies.

6 Requests (Part B)

The requests for ‘Assignment 1 (Part B)’ are the followings:

- Apply the procedure developed within Part A to the provided experimental data, to identify the modal parameters (natural frequencies, damping ratios and mode shapes) of the first two axial modes.
- Check the quality of the identification comparing the identified FRFs and the experimental ones.
- Plot a diagram showing the identified mode shapes with the indication of the corresponding natural frequencies and damping ratios.

7 Data Analysis

In this section, the data collected during the experimental campaign are analyzed. The data are processed exactly as described in the previous section (see Section 4), and the identified parameters are used to compute the numerical FRFs and the mode shapes of the system.

In particular, by plotting the given data (which are the experimental FRFs coming from impact test performed on a rail wheel and sampled in different angular position), we can clearly see that multiple peaks are present (see Figure 12). However, this study will be focused on the first two peaks only, given that considering the real system from which data are acquired, those are the ones of interest.

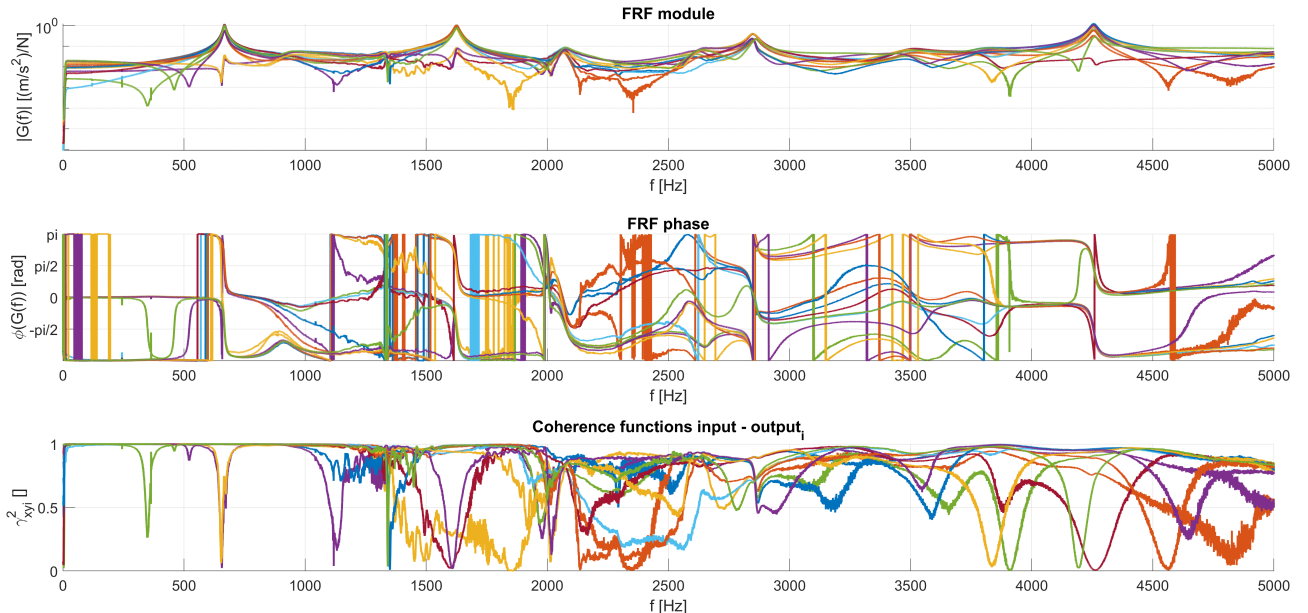


Figure 12: FRFs and coherence functions of the system.

7.1 First peak

Modal parameters analysis applied to the first peak of the FRFs allows us to identify the natural frequency and the damping ratio of the first mode. The identified parameters are reported in Table 4.

| | |
|-------------|---------|
| f_i [Hz] | 667.324 |
| ξ_i [%] | 0.75 % |

Table 4: First peak modal parameters.

From a graphical point of view, the experimental and numerical FRFs are compared in Figure 13.

7.2 Second peak

Modal parameters analysis applied to the second peak of the FRFs allows us to identify the natural frequency and the damping ratio of the second mode. The identified parameters are reported in Table 5.

| | |
|------------------|----------|
| $f_i[\text{Hz}]$ | 1625.312 |
| $\xi_i[\%]$ | 0.59 % |

Table 5: Second peak modal parameters.

From a graphical point of view, the experimental and numerical FRFs are compared in Figure 14.

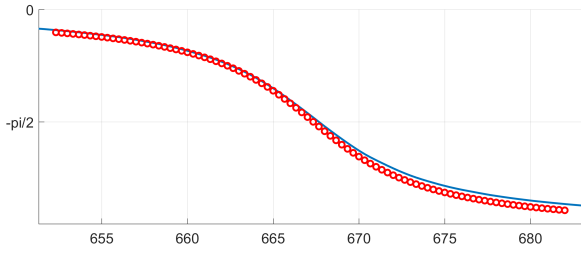
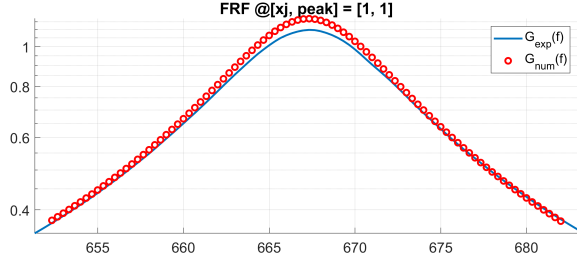


Figure 13: First peak FRFs comparison.

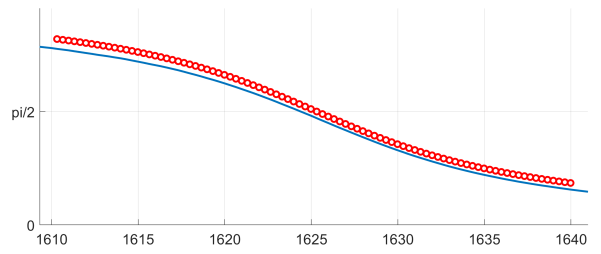
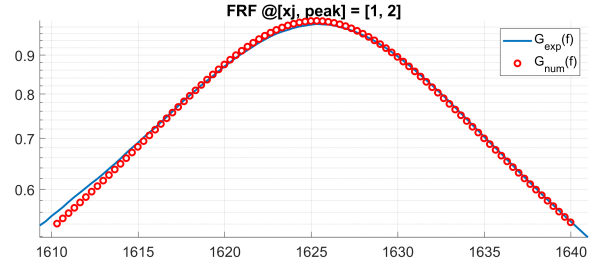


Figure 14: Second peak FRFs comparison.

8 Final Results (mode shapes visualization)

In this section, the mode shapes identified from the experimental data are reported.

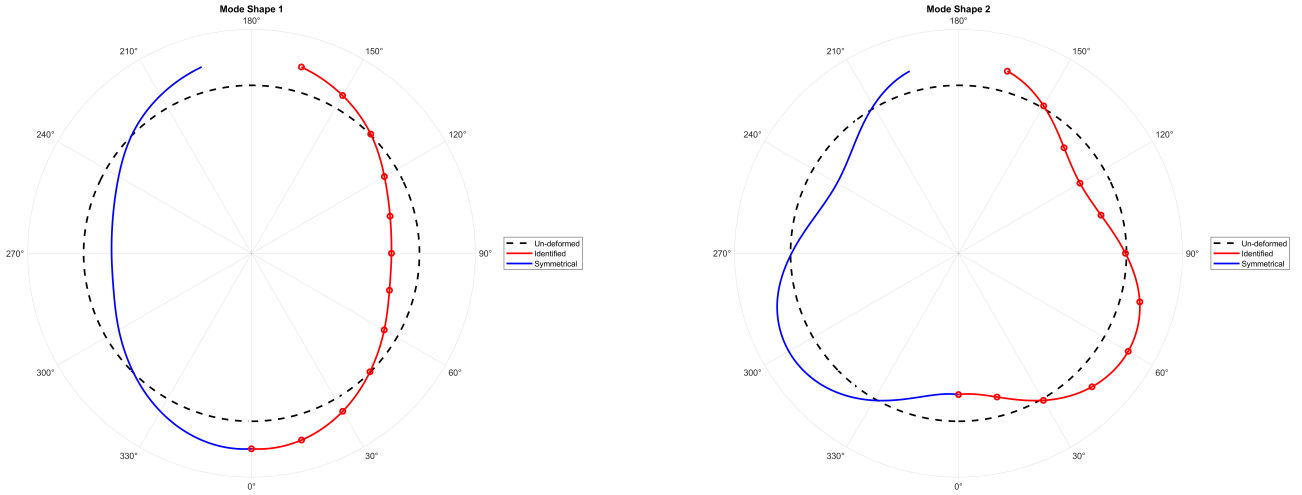


Figure 15: Identified (numerically) first two mode shapes of the system.

These graphs represent axial displacements relative to the undeformed system. The farther the colored lines are from the black dashed line, the greater the axial deformation in that region. Additionally, the position of the colored lines relative to the black dashed line (either outside or inside) indicates the direction of the deformation with respect to the undeformed plane of the system.

The first mode shape (Figure 15, left) can also be visualized in a 3D way that to a FEA simulation performed in [1].

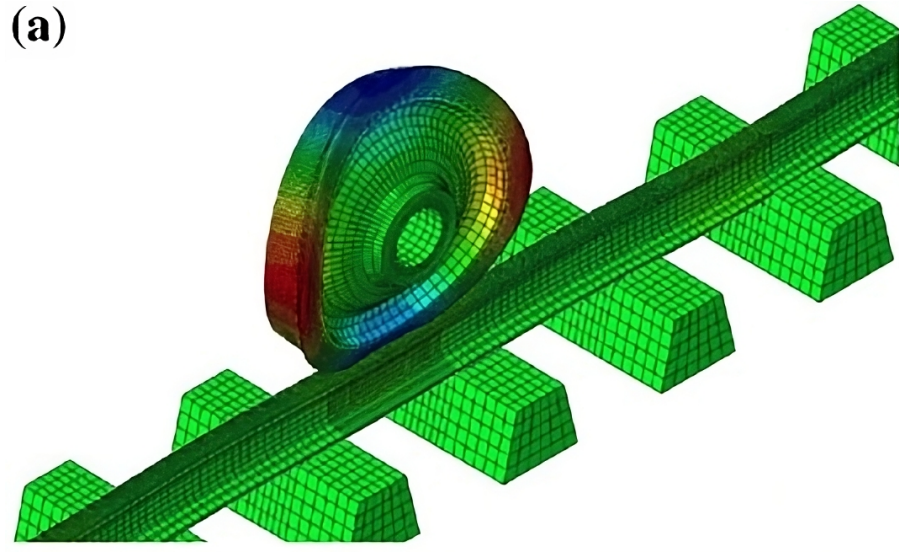


Figure 16: First mode shape of the system visualized in a 3D way. Credit to [1].

As a final remark, we report in Table 6 the identified parameters for the first two mode shapes of the system.

| Mode | Frequency [Hz] | Damping ratio [%] |
|------|----------------|-------------------|
| 1 | 667.324 | 0.75 % |
| 2 | 1625.312 | 0.59 % |

Table 6: Identified parameters for the first two mode shapes of the system.

References

- [1] Guangxiong Chen, Xiaolu Cui, and W. Qian. Investigation into rail corrugation in high-speed railway tracks from the viewpoint of the frictional self-excited vibration of a wheel–rail system. *Journal of Modern Transportation*, 24, 04 2016.

Advanced Dynamics of Mechanical Systems
Assignment 2

Tommaso Bocchietti 10740309

A.Y. 2023/24



POLITECNICO
MILANO 1863

Contents

| | |
|--|-----------|
| 1 Requests | 4 |
| 2 FE model | 4 |
| 2.1 Geometry and material properties | 5 |
| 2.2 Matrices assembly | 5 |
| 2.3 Modal analysis | 6 |
| 3 FRFs of the structure | 8 |
| 3.1 FRFs computation | 8 |
| 3.2 FRFs examples | 9 |
| 3.2.1 Direct method - Vertical force A to Vertical displacement A and Horizontal displacement B | 9 |
| 3.2.2 Direct vs. Modal superposition method - Vertical force A to Horizontal displacement B | 10 |
| 3.2.3 Direct method - Vertical force C to Vertical reaction force O2 | 10 |
| 4 Static responses of the structure | 11 |
| 4.1 Displacement approach | 11 |
| 4.2 Acceleration approach | 12 |
| 4.3 Comparison of the two methods | 13 |
| 5 Response due to moving loads | 13 |
| 5.1 Trapezoidal motion profile | 13 |
| 5.2 Initial conditions | 14 |
| 5.3 Results | 14 |
| 5.3.1 Initial condition 1 | 14 |
| 5.3.2 Initial condition 2 | 15 |

List of Figures

| | |
|---|----|
| 1 Harbour crane | 4 |
| 2 Harbour crane scheme. Node naming: $[A, B, C, D, O2] = [\#9, \#14, \#1, \#7, \#15]$ | 5 |
| 3 Firsts mode shapes of the FE model. Scale factor = 10. | 7 |
| 4 FRF computed using the direct method - Vertical force A to Vertical displacement A and Horizontal displacement B | 9 |
| 5 FRF computed using the direct method and modal superposition method - Vertical force A to Horizontal displacement B | 10 |
| 6 FRF computed using the direct method - Vertical force C to Vertical reaction force O2 | 11 |
| 7 Displacement method for distributed loads. | 11 |
| 8 Comparison of the static responses of the structure computed using the displacement approach and the acceleration approach. | 13 |
| 9 Dynamic response of the structure due to the moving load (initial condition 1, mode shapes considered 3). | 14 |
| 10 Dynamic response of the structure due to the moving load (initial condition 1, mode shapes considered 50). | 15 |
| 11 Dynamic response of the structure due to the moving load (initial condition 2, mode shapes considered 3). | 15 |
| 12 Dynamic response of the structure due to the moving load (initial condition 2, mode shapes considered 50). | 15 |

List of Tables

| | |
|---|---|
| 1 Parameters of the structure | 5 |
|---|---|

Listings

| | | |
|---|--|----|
| 1 | MATLAB code to compute the natural frequencies and mode shapes of the system. | 7 |
| 2 | MATLAB code to compute the FRFs of the structure using the direct method. | 8 |
| 3 | MATLAB code to compute the FRFs of the structure using the modal superposition method. . . | 8 |
| 4 | Displacement approach to compute the static responses of the structure. | 12 |
| 5 | Acceleration approach to compute the static responses of the structure. | 12 |

1 Requests

Considering a harbour crane represented in Figure 1, the requests for ‘Assignment 2’ are the followings:

- Define a FE model of the structure in the 0-8 Hz frequency range considering a safety factor equal to 2.
- Calculate the structure’s natural frequencies and vibration modes up to the 3rd mode. Plot the mode shapes with the indication of the associated natural frequencies.
- Calculate the structure frequency response functions which relate the input force applied at position A in vertical direction to the outputs vertical displacement at point A and horizontal displacement at point B. Assume the input force to vary in the 0-8 Hz frequency range and set the frequency resolution to 0.01 Hz.
- Using the modal superposition approach and considering the structure’s first two modes, calculate the frequency response functions which relate the same input force of question 3 (vertical force applied in node A) to the horizontal displacement of node B. Plot the corresponding magnitude and phase diagrams superimposed to those obtained in item 3. Point out the differences and comment the results.
- Calculate the structure frequency response function relating the input force applied at position C in vertical direction to the output axial force in the right column evaluated at point O2. Assume the input force to vary in the 0-8 Hz frequency range and set the frequency resolution to 0.01 Hz.
- Compute the static response of the structure due to the weight of the entire structure. Plot the deformed shape of the structure compared to the undeformed configuration and compute the value of the maximum deflection.
- Optional - Calculate the vertical displacement time history of point A, taking into account a moving load traveling between points D and A. The load begins with zero initial velocity, uniformly accelerates over the first 8 meters, keeps a constant velocity over the next 8 meters and then decelerates until reaching point A with null velocity. Total time to travel from D to A is 20s.



Figure 1: Harbour crane

2 FE model

In the following subsections, we will describe the Finite Element Model (FEM) of the harbour crane and discuss some key aspects of the model, such as the geometry and material properties and the assembly of the mass and stiffness matrices. We will also discuss the results obtained from the modal analysis of the system.

2.1 Geometry and material properties

At first the FEM model was created considering a safety factor of 2 and a maximum operating frequency range of $0 - 8[\text{Hz}]$.

From theory, we know that in a FEM model the geometry and in particular the length of the elements is determinant when it comes to the accuracy of the results, given that a too coarse mesh can lead to inaccurate results, while a too fine mesh can lead to a high computational cost. Because of this, the maximum length of the single elements was determined as:

$$L_{\max} = \sqrt{\frac{\pi^2}{\eta\Omega_{\max}} \sqrt{\left(\frac{EJ}{m}\right)_{\min}}} \approx 12 \quad [\text{m}] \quad (1)$$

Once the model has been discretized and the geometrical and material properties have been assigned to each element based on the suggested values reported in Table 1, the model was imported in adequate MATLAB data structures.

The output of this first step is a schematized version of the harbour crane, as shown in Figure 2.

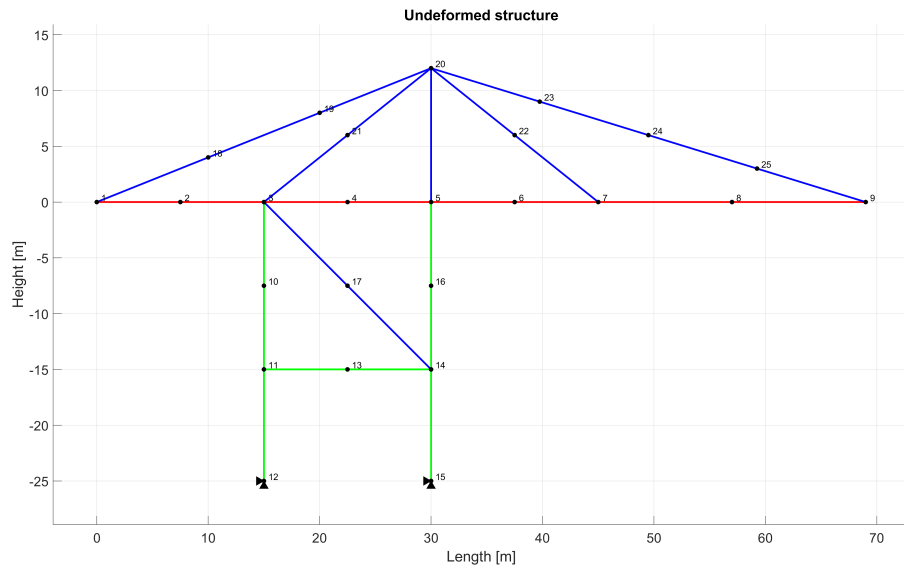


Figure 2: Harbour crane scheme. Node naming: $[\mathbf{A}, \mathbf{B}, \mathbf{C}, \mathbf{D}, \mathbf{O2}] = [\#9, \#14, \#1, \#7, \#15]$

As suggested/requested by the assignment, the harbour crane was modelled as a 2D frame structure composed of beam elements. As an assumption, the joints **A** and **C** were assumed to be rigid connections, even if in reality those elements are usually not capable of transmit bending moments, but only axial forces (hinge connections type). This assumption was made to simplify the model and the analysis. However, the model could be easily modified to include the possibility of free relative rotations in those joints by adding another degree of freedom to the system.

With respect to the schematic representation of the crane of Figure 2, the parameters of the structure are provided in Table 1.

| | m [kg/m] | EA [N] | EJ [Nm^2] |
|-------------|-----------------------------------|--------------------------|-----------------------------|
| Red beams | 312 | $8.2E9$ | $1.4E9$ |
| Green beams | 200 | $5.4E9$ | $4.5E8$ |
| Blue beams | 90 | $2.4E9$ | $2.0E8$ |

Table 1: Parameters of the structure

For the rest of the analysis, we will assume a proportional damping matrix $[C] = \alpha[M] + \beta[K]$ with $\alpha = 0.01[\frac{1}{s}]$ and $\beta = 2E - 4[s]$

2.2 Matrices assembly

Once the geometrical and material properties of the structure are known, it is possible to assemble the mass and stiffness matrices of the system, and empirically also the damping matrix.

A common approach to assemble the mass and stiffness matrices is to loop over all the elements of the structure and to add the contribution of each element to the global matrices. To do so, it is necessary to calculate the element matrices, which are the mass and stiffness matrices of each element in the local reference frame. Then, the element matrices are transformed into the global reference frame and added to the global matrices.

The mass matrix of an element is computed as:

$$[M_{el}] = \int_0^L \mathbf{N}^T \rho A \mathbf{N} dx \quad (2)$$

Where ρ is the mass density of the material, A is the cross-sectional area of the element, N is the shape function matrix, and L is the length of the element.

The stiffness matrix of an element is computed as:

$$[K_{el}] = \int_0^L \mathbf{B}^T [E] \mathbf{B} dx \quad (3)$$

Where $[E]$ is the elasticity matrix of the material, \mathbf{B} is the strain-displacement matrix, and L is the length of the element.

Once the element matrices are computed, they are transformed into the global reference frame using the transformation matrix $[Q]$:

$$[M_{el}] = [Q]^T [M_{el}] [Q] \quad (4)$$

$$[K_{el}] = [Q]^T [K_{el}] [Q] \quad (5)$$

Where $[Q]$ is the transformation matrix of the element, which is computed as:

$$[Q] = \begin{bmatrix} \cos(\theta) & \sin(\theta) & 0 & 0 & 0 & 0 \\ -\sin(\theta) & \cos(\theta) & 0 & 0 & 0 & 0 \\ 0 & 0 & 1 & 0 & 0 & 0 \\ 0 & 0 & 0 & \cos(\theta) & \sin(\theta) & 0 \\ 0 & 0 & 0 & -\sin(\theta) & \cos(\theta) & 0 \\ 0 & 0 & 0 & 0 & 0 & 1 \end{bmatrix} \quad (6)$$

Where θ is the angle between the local and global reference frames.

Finally, the element matrices are added to the global matrices considering the contribution of each element to the corresponding global degrees of freedom of the system:

$$[M] = [M] + [Q]^T [M_{el}] [Q] \quad (7)$$

$$[K] = [K] + [Q]^T [K_{el}] [Q] \quad (8)$$

The damping matrix can be computed similarly, using the proportional damping matrix $[C] = \alpha[M] + \beta[K]$.

Matrices partitioning As a preference choice (even if not strictly necessary), the structure geometry definition and in particular the node and degree of freedom numbering, were performed in order to have the following partitioning of the matrices:

$$[M] = \begin{bmatrix} [M_{FF}] & [M_{FC}] \\ [M_{CF}] & [M_{CC}] \end{bmatrix} \quad [K] = \begin{bmatrix} [K_{FF}] & [K_{FC}] \\ [K_{CF}] & [K_{CC}] \end{bmatrix} \quad [C] = \begin{bmatrix} [C_{FF}] & [C_{FC}] \\ [C_{CF}] & [C_{CC}] \end{bmatrix} \quad (9)$$

Where the subscripts F and C refer to the free and constrained degrees of freedom, respectively.

2.3 Modal analysis

To understand how the structure behaves when excited by a force, it is necessary to calculate the natural frequencies and the mode shapes of the system.

As usual, the natural frequencies are the eigenvalues of the unloaded (free) system, while the mode shapes are the eigenvectors. Since we are dealing with a discretized system, we can expect as many natural frequencies as the number of degrees of freedom of the system.

In this phase, we can ignore the damping matrix, since its contribution is negligible in the calculation of the natural frequencies and mode shapes, so that the eigenvalues problem to be solved became:

$$[M_{FF}] \ddot{\mathbf{X}} + [0] \dot{\mathbf{X}} + [K_{FF}] \mathbf{X} = 0 \quad (10)$$

Which indeed brings to the standard eigenvalues problem:

$$(\omega^2[I] - [M_{FF}]^{-1}[K_{FF}])\mathbf{X} = 0 \quad (11)$$

Solvable in MATLAB with the following code:

```

1 [M, K] = assembly(incid, l, m, EA, EJ, gamma, idb);
2 C = 1e-1 * M + 2.0e-4 * K;
3
4 M_FF = M(1:ndof, 1:ndof);
5 C_FF = C(1:ndof, 1:ndof);
6 K_FF = K(1:ndof, 1:ndof);
7
8 [mode_shapes, omega_square] = eig(M_FF\K_FF);
9 omega_nat = sqrt(diag(omega_square));

```

Listing 1: MATLAB code to compute the natural frequencies and mode shapes of the system.

As we have said before, from the code above we expect to have as many natural frequencies as the number of degrees of freedom of the system. However, we always have to keep in mind the real physical representation of the problem. In this case, the model represents a harbour crane, which is a machine that typically works or is subjected to forces having a low frequency range. As suggested by the assignment, our interest is in the $0 - 8$ [Hz] frequency range.

Therefore, it's reasonable to expect that just the first few natural frequencies are significant, while the others (even if present also in the real structure) are not excited in a way that can be considered relevant for the analysis and can be neglected.

In the following, we will show the first four mode shapes of the system and the corresponding natural frequencies.

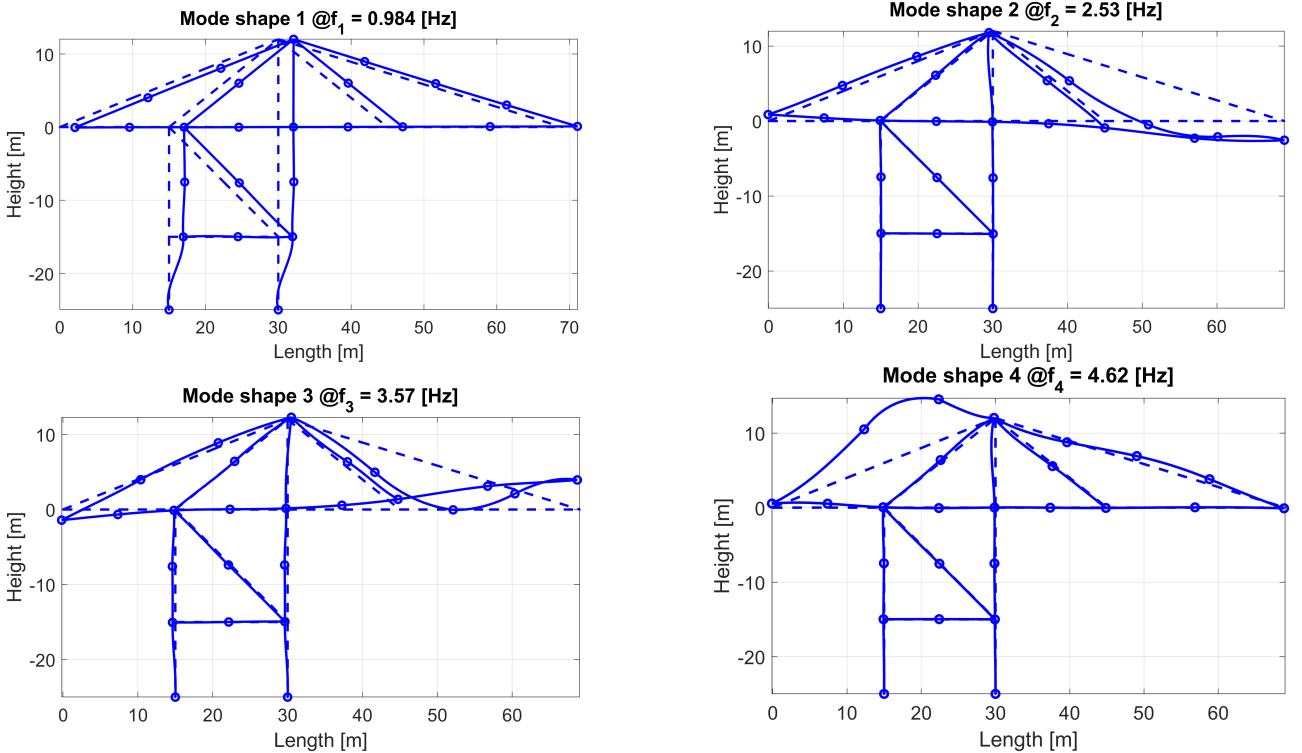


Figure 3: Firsts mode shapes of the FE model. Scale factor = 10.

Notice how the first mode shape is almost a rigid body motion, while the others are more complex and involve bending of the arm's beams elements. This can be easily explained by the fact that the equivalent stiffness of the first mode shape is due to only the lateral displacement of the two supporting beam elements that connect the structure to the ground. This, however, won't be a real problem given that this mode shape is generally not excited by the forces acting on the crane that are usually in the vertical direction.

When we will perform the dynamic analysis of the system, we will see that the mode shapes involved in the response of the system are from the second one on, since they involve the bending of the arm's elements, which are directly excited by the vertical forces due to the carrying of the load.

3 FRFs of the structure

Once the model has been defined and the natural frequencies and mode shapes have been calculated, the next step is to compute the Frequency Response Functions (FRFs) of the structure. The FRFs are a fundamental tool in the analysis of dynamic systems, as they provide a quantitative measure of the system's response to an external excitation as a function of frequency.

3.1 FRFs computation

To compute the FRFs, we can either use the direct method or the modal superposition method.

Direct method The direct method consists of solving the classical equation of motion considering all the degrees of freedom of the system (or equivalently, all the possible mode shapes of the system).

The equation of motion for a linear system can be written as:

$$[M_{FF}]\ddot{\mathbf{X}} + [C_{FF}]\dot{\mathbf{X}} + [K_{FF}]\mathbf{X}_F = \mathbf{F}_F \quad (12)$$

Where \mathbf{X}_F is the displacement vector of the free degree of freedom and \mathbf{F}_F is the external force vector (acting on the free degrees of freedom of the system).

To solve this equation, we can work in the complex plane and then consider the real part of the solution to obtain the physical response of the system.

By doing so, the FRF can be computed as:

$$\mathbf{H}(\Omega) = (-\Omega^2[M_{FF}] + j\Omega[C_{FF}] + [K_{FF}])^{-1}\mathbf{F}_F \quad (13)$$

Where $\mathbf{H}(\omega)$ is the FRF relating the particular set of forces \mathbf{F}_F applied in one or more nodes, to the response of any other (free) node of the structure.

In MATLAB, the FRFs based on direct approach can be implemented as follows:

```

1 % Here we compute the FRFs due to a vertical force applied to node A with module 1
2 F_F(node_A_vertical) = 1;
3
4 FRF_direct_approach = zeros(size(M_FF, 1), length(omega_vet));
5 for ii = 1:length(omega_vet)
6     FRF_direct_approach(:, ii) = (-omega_vet(ii)^2 * M_FF + 1j*omega_vet(ii) * C_FF +
7         K_FF) \ F_F;
8 end

```

Listing 2: MATLAB code to compute the FRFs of the structure using the direct method.

Modal superposition method The modal superposition method is an alternative approach to compute the FRFs of a structure. It's based on the modal decomposition of the system response, which allows us to reduce the size of the problem and so the computational efforts required.

The idea behind this approach, is to consider as negligible the contribution of the higher modes of the system, and to focus only on the first few modes that are significant in the frequency range of interest.

Having this hypothesis in mind, we can proceed with the orthogonalization of the global matrices based on the first n mode shapes of the system, which indeed cause a significant reduction in size of the given problem. As an example, if we consider the first $n = 5$ mode shapes of the system, all the matrices will be reduced to a 5×5 size, and FRFs matrix will also be reduced to a $5 \times \text{length}(\omega_{vector})$.

This approach, in general, is more efficient than the direct method, especially when the number of degrees of freedom of the system is high. However, as we can imagine, the accuracy of the results will strongly depend on the number of modes considered in the analysis and the frequency and position of the forces acting on the structure.

In MATLAB, the FRFs based on modal superposition can be implemented as follows:

```

1 % To observe the approximation introduced, we consider only 2 modes
2 % Here we compute the FRFs due to a vertical force applied to node A with module 1
3
4 F_F(node_A_vertical) = 1;
5
6 Phi_reduced = mode_shapes(:, 1:2);
7 M_FF_modal_reduced = Phi_reduced' * M_FF * Phi_reduced;

```

```

8 C_FF_modal_reduced = Phi_reduced' * C_FF * Phi_reduced;
9 K_FF_modal_reduced = Phi_reduced' * K_FF * Phi_reduced;
10 F_F_modal = Phi_reduced' * F_F;
11
12 FRF_modal_approach = zeros(size(M_FF_modal_reduced, 1), length(omega_vet));
13 for ii = 1:length(omega_vet)
14     FRF_modal_approach(:, ii) = (-omega_vet(ii)^2 * M_FF_modal_reduced + 1i*omega_vet(ii)
15 ) * C_FF_modal_reduced + K_FF_modal_reduced) \ F_F_modal;
16 end
17
FRF_modal_approach = Phi_reduced * FRF_modal_approach;

```

Listing 3: MATLAB code to compute the FRFs of the structure using the modal superposition method.

Notice that, even if the size of the FRFs matrix is reduced, the final result must be projected back to the original space to obtain the physical response of the system.

The transformation between one set of coordinates and the other is performed via the matrix $[\Phi]$ composed by the mode shapes of the system (in this case, the first n mode shapes).

3.2 FRFs examples

In this section we will show some examples of FRFs computed for the harbour crane model, and, for some of them, we will discuss the results obtained using both the direct method and the modal superposition method.

3.2.1 Direct method - Vertical force A to Vertical displacement A and Horizontal displacement B

In this example, we compute the FRF relating the vertical displacement of node **A** and the horizontal displacement of node **B** to the vertical force applied to node **A**. The FRFs are computed using the direct method, considering all the degrees of freedom of the system.

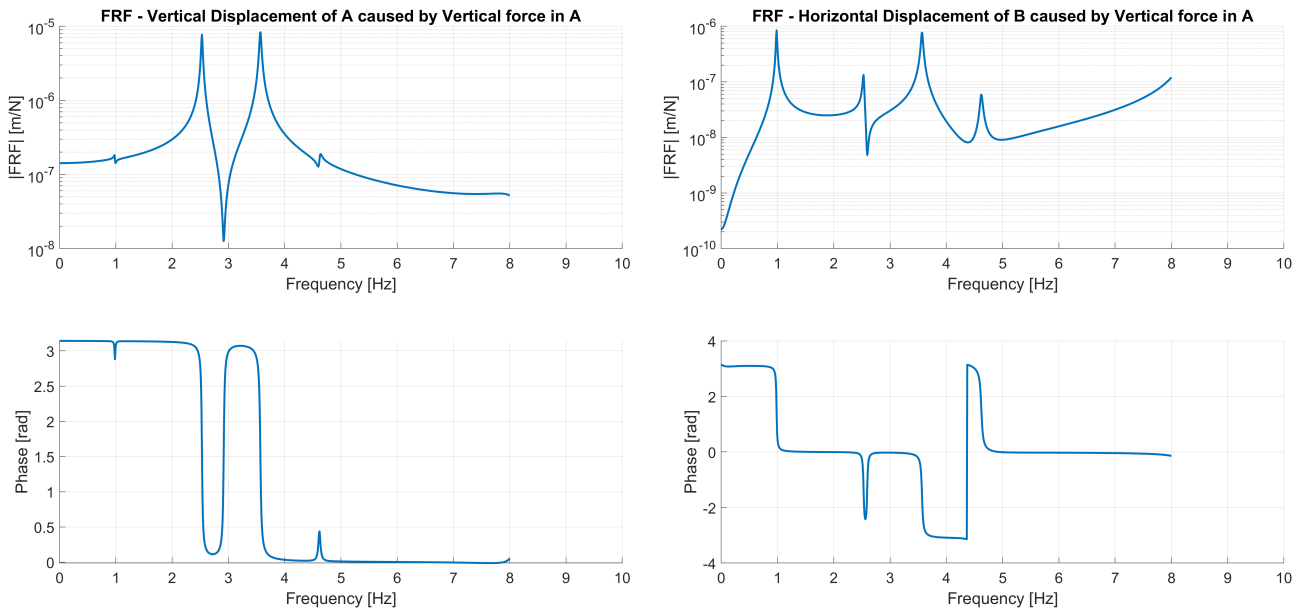


Figure 4: FRF computed using the direct method - Vertical force **A** to Vertical displacement **A** and Horizontal displacement **B**.

From the FRFs shown in Figure 4, we can observe that in the considered frequency range ($0 - 8[\text{Hz}]$), the vertical displacement of node **A** is more sensitive to the vertical force applied to node **A** than the horizontal displacement of node **B**.

Moreover, as expected, the resonance peaks in the FRFs correspond to the natural frequencies of the system found during modal analysis (see Section 2.3).

Interestingly, both FRFs exhibit an anti-resonance peak between the third and fourth natural frequencies (at $\approx 2.91[\text{Hz}] \rightarrow 18.28[\text{rad/s}]$), which indicates that the system's response to the excitation is minimized at that frequency. In other words, at that specific excitation frequency, node **A** became stationary and any force applied

at the corresponding frequency will not excite the system (no energy can flow from the force to the structure, null virtual work).

3.2.2 Direct vs. Modal superposition method - Vertical force A to Horizontal displacement B

In this example, we compute the FRF relating the horizontal displacement of node **B** to the vertical force applied to node **A**. We compare the results obtained using the direct method and the modal superposition method.

In order to have a significant comparison of the effect of the reduction of the number of modes considered in the analysis, we will consider only the first two mode shapes of the system in the modal superposition method ($n = 2$).

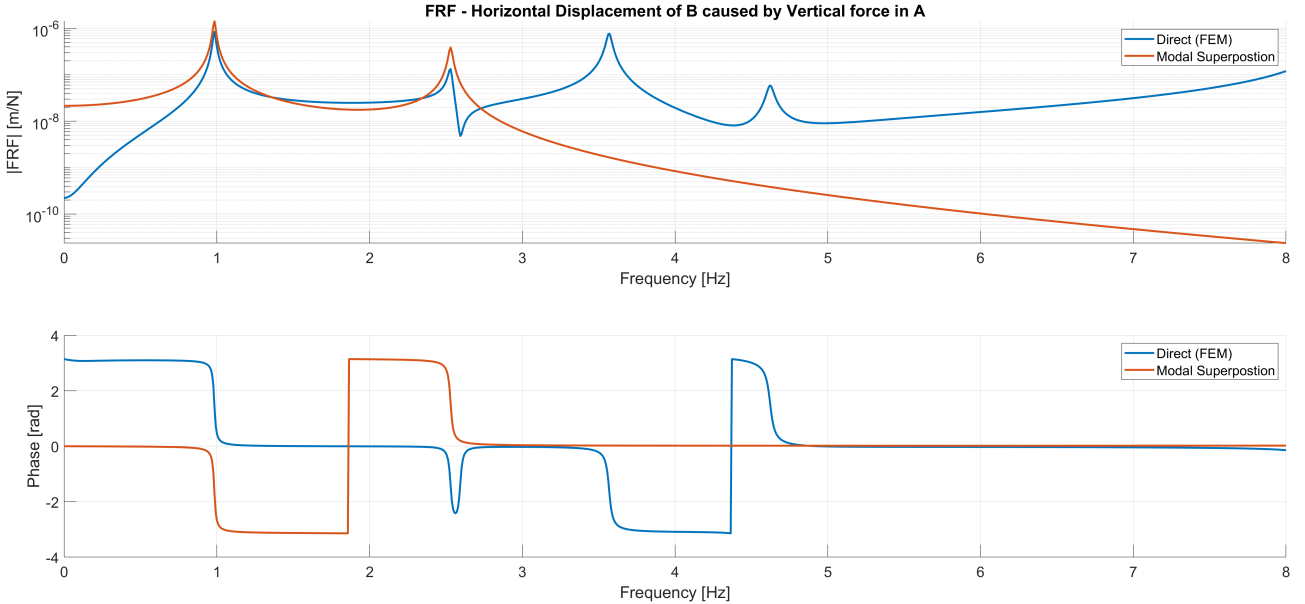


Figure 5: FRF computed using the direct method and modal superposition method - Vertical force **A** to Horizontal displacement **B**.

From the FRFs shown in Figure 5, we can observe that the results obtained using the direct method and the modal superposition method are in good agreement only around the considered natural frequencies of the system. As we move away from the peaks, the results start to diverge.

This behavior is expected since the modal superposition method considers only the first two mode shapes of the system, which may not capture the full dynamic behavior of the structure. On the other hand, the direct method considers all the degrees of freedom of the system, providing a more accurate representation of the system's response to the excitation (at the cost of higher computational effort).

3.2.3 Direct method - Vertical force C to Vertical reaction force O2

In this example, we compute the FRF relating the vertical reaction force at node **O2** to the vertical force applied to node **C**. The FRF is computed using the direct method, considering all the degrees of freedom of the system.

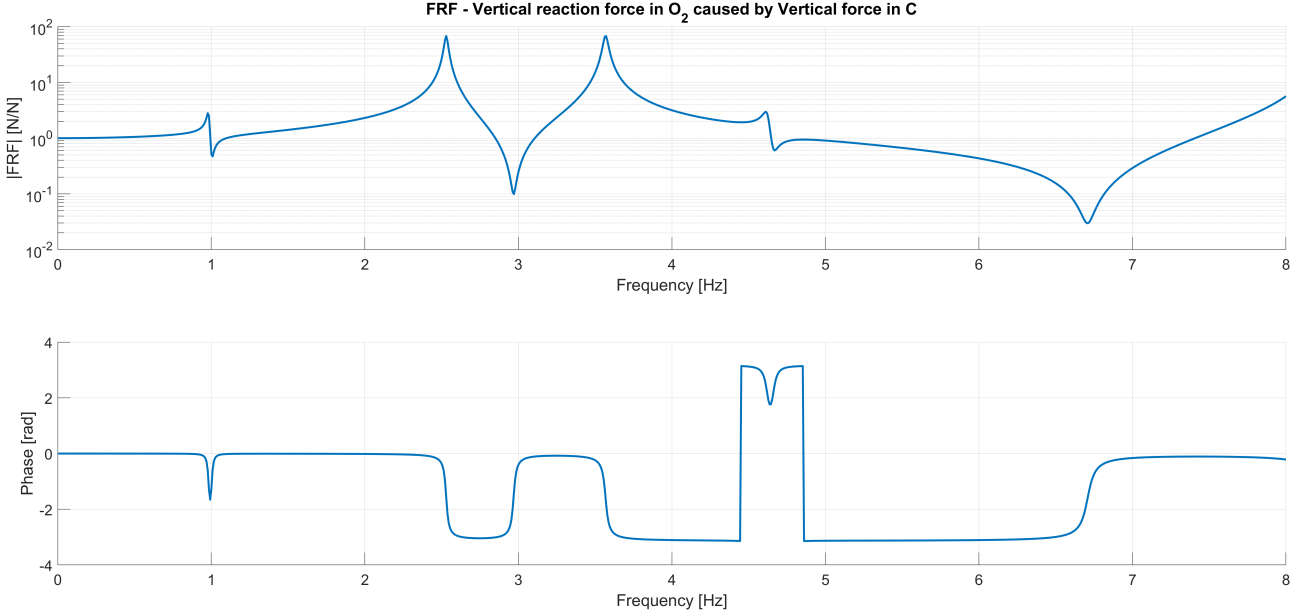


Figure 6: FRF computed using the direct method - Vertical force **C** to Vertical reaction force **O2**

Notice that reaction forces are computed in two consecutive steps: first, using the direct method the displacement in time of each node is computed obtaining the vector $\mathbf{q}(t)$, then the reaction forces are computed by substituting the displacement vector in the equation of motion relative to the constrained nodes, obtaining the reaction forces vector $\mathbf{R}(t)$.

4 Static responses of the structure

In this section, we will focus on the computation of the static responses of the structure, that are the displacements of the structure when subjected to a static load.

Again, as in many other engineering problems, we can approach this problem in at least a couple of different ways. In the following, we will explain how to compute the static responses of the structure using both a displacement approach and an acceleration approach.

Notice that the two method differs only in the way the global force vector \mathbf{F}_F is assembled. In the end, once \mathbf{F}_F is known, both methods will solve the steady state version of the equation of motion:

$$[K_{FF}]\mathbf{X}_F = \mathbf{F}_F \quad (14)$$

Where $[K_{FF}]$ is the stiffness matrix, \mathbf{X}_F is the vector of displacements and \mathbf{F}_F is the global force vector, all referred to the free degrees of freedom of the nodes.

4.1 Displacement approach

The displacement approach consists of assembling the global force vector \mathbf{F}_F based on the ‘displacement method’ used in structural mechanics.

In particular, if the structure is subjected to a distributed static load (as in the case of the gravity load), we know that the nodal forces on a single beam element can be computed as:

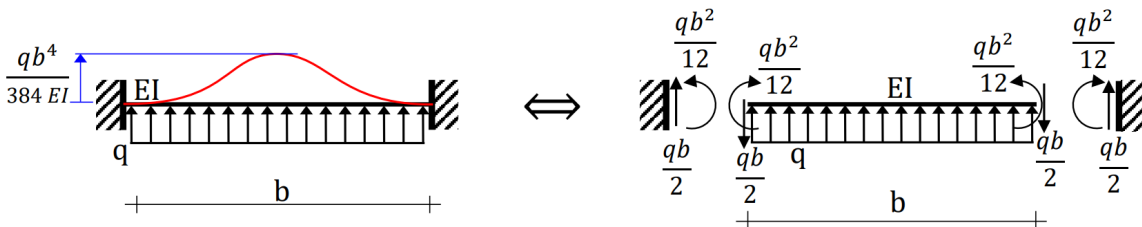


Figure 7: Displacement method for distributed loads.

From the figure above, we can obtain the coefficients needed to compute the equivalent nodal forces due to a distributed load along the element.

By using proper change in the reference system (by rotational matrices), it's possible to build the equivalent global force vector \mathbf{F}_F , which can be seen as the equivalent effect on the node of the structure due to the distributed load.

Finally, we can solve the equation of motion 14 to obtain the displacements of the structure.

In MATLAB, the displacement approach can be implemented as follows:

```

1 % Displacement approach.
2 F_F_global = zeros(3*nnod, 1);
3
4 for ii = 1:nbeam
5
6 [R, Q] = compute_rotational_matrices(gamma(ii));
7
8 % Here we are neglecting the possibility of a distributed momentum
9 % load. Just distributed force loads are considered.
10 elemental_distributed_load = R(1:2, 1:2)' * [0 -9.81 * m(ii)]';
11
12 elemental_equivalent_nodal_load = [
13     l(ii)/2 0
14     0     l(ii)/2
15     0     l(ii)^2/12
16     l(ii)/2 0
17     0     l(ii)/2
18     0     -l(ii)^2/12
19 ] * elemental_distributed_load;
20
21 global_equivalent_nodal_load = Q * elemental_equivalent_nodal_load;
22
23 F_F_global(incid(ii, :)) = F_F_global(incid(ii, :)) + global_equivalent_nodal_load;
24
25 end
26
27 X_gravity_displacement_approach = K_FF \ F_F_global(1:ndof);
```

Listing 4: Displacement approach to compute the static responses of the structure.

4.2 Acceleration approach

The acceleration approach instead, consists of assembling the global force vector \mathbf{F}_F based on the idea that the structure (since it has been discretized), can be seen as a system of masses connected by springs and dampers. Because of this, a distributed acceleration load can be directly transformed into a series of nodal forces by solving the second Newton's law for each node of the structure.

In particular, the nodal forces can be computed as:

$$\mathbf{F}_F = [M_{FF}] \cdot \mathbf{a} \quad (15)$$

Where $[M_{FF}]$ is the mass matrix of the structure and \mathbf{a} is the vector of accelerations acting on each degree of freedom of the structure.

Finally, we can solve the equation of motion 14 to obtain the displacements of the structure.

In MATLAB, the acceleration approach can be implemented as follows:

```

1 % Acceleration approach.
2 x_dot_dot = zeros(ndof, 1);
3 x_dot_dot(idb(:, 2)) = -9.81;
4
5 F_F_nodal = M * x_dot_dot;
6
7 X_gravity_acceleration_approach = K_FF \ F_F_nodal(1:ndof);
```

Listing 5: Acceleration approach to compute the static responses of the structure.

4.3 Comparison of the two methods

As we can see from Figure 8, the two methods give the same results. This is expected given that the acceleration approach is just a derivation of the displacement approach, since the mass matrices M and the stiffness matrices K are just an implementation of the displacement and/or the force method used to solve structures.

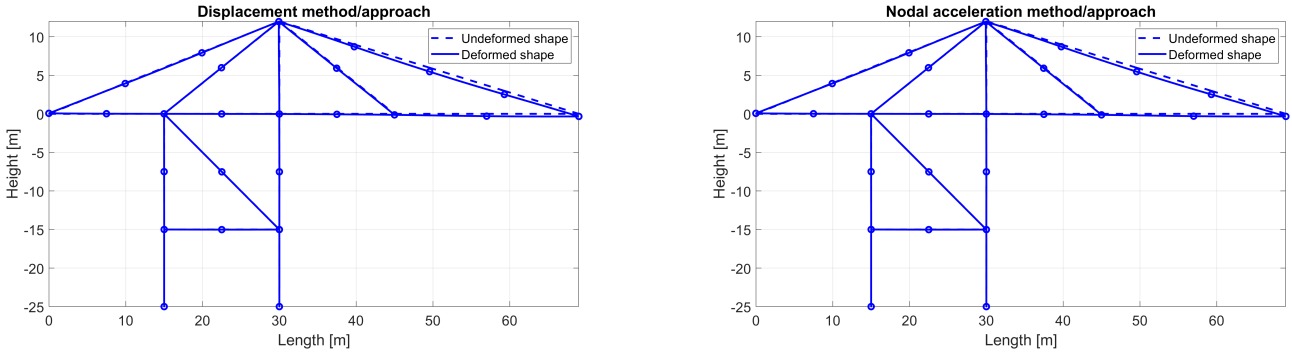


Figure 8: Comparison of the static responses of the structure computed using the displacement approach and the acceleration approach.

5 Response due to moving loads

Finally, we can simulate a real working condition for the harbour crane, by applying a moving load on the structure.

In particular, we can consider a mass of $m = 45[T] = 45E3[Kg]$ moving along the crane's arm, starting in correspondence of node **D** and moving towards node **A** (tip of the arm crane).

5.1 Trapezoidal motion profile

As for the motion type of the mass along the x axis, we can consider a trapezoidal velocity profile, with a constant acceleration phase, a constant velocity phase, and a constant deceleration phase. In particular, if we consider the total distance covered by the mass as $L = 24[m]$ and a total time of $T = 20[s]$, we can compute both the accelerations ($a_{acc} = |a_{dec}| = a$), velocity (v_{max}), and the time duration of each phase (t_1 , t_2 and t_3):

$$\begin{cases} L = \frac{1}{2} \cdot a \cdot t_1^2 + v_{max} \cdot t_2 + \frac{1}{2} \cdot |a| \cdot t_3^2 \\ T = t_1 + t_2 + t_3 \end{cases} \quad (16)$$

By solving the system of equations, we can find the following values:

$$\begin{cases} a = 0.25[m/s^2] \\ v_{max} = 2[m/s] \\ t_1 = 8[s] \\ t_2 = 4[s] \\ t_3 = 8[s] \end{cases} \quad (17)$$

Once the position of the load over time is computed, we must compute the equivalent nodal forces that is applied to the structure because of the load.

For simplicity, we neglect any nodal momentum, and we just consider the vertical nodal force. By doing so, we can compute the equivalent nodal force by solving the following equations:

$$\xi = \frac{x - x_1}{x_2 - x_1} \quad (18)$$

$$\mathbf{F}_{\text{F,eq,left}} = m \cdot g \cdot \xi \quad (19)$$

$$\mathbf{F}_{\text{F,eq,right}} = m \cdot g \cdot (1 - \xi) \quad (20)$$

Where x is the position of the mass, x_1 and x_2 are the position of the two nodes that are closest to the mass, and g is the gravity acceleration.

Once the nodal forces are known for each time step, we can compute the nodal displacements by solving the partial differential equation that describes the motion of the structure:

$$[M_{FF}] \cdot \ddot{\mathbf{X}}(t) + [C_{FF}] \cdot \dot{\mathbf{X}}(t) + [K_{FF}] \cdot \mathbf{X}(t) = \mathbf{F}_{\mathbf{F},\text{eq}}(t) \quad (21)$$

Where $[M_{FF}]$, $[C_{FF}]$ and $[K_{FF}]$ are the mass, damping and stiffness matrices of the structure, \mathbf{X} is the nodal displacement vector, and $\mathbf{F}_{\mathbf{F},\text{eq}}$ is the equivalent nodal force vector.

To solve the equation, we must rely on a numerical method, such as the ‘Runge-Kutta’ method, that allows us to solve the equation for each time step.

5.2 Initial conditions

One important aspect about this type of analysis is the initial conditions of the structure.

In particular, we can consider two different initial conditions:

- **Initial condition 1:** the structure is in its undeformed configuration, and the load is suddenly added to the structure.
- **Initial condition 2:** the structure is in its deformed configuration due to the static loads of the mass, which then starts to move along the x axis.

As we can imagine, the first set of initial conditions will lead to a much more complex dynamic response since it will be the superposition of the fast dynamic response due to the sudden addition of the load (oscillatory behavior) and the slow dynamic response due to the moving load. On the other hand, the second set of initial conditions will lead to an almost steady dynamic response, since the structure starts from a condition much more near (in terms of displacements) to the final condition.

5.3 Results

In this section, we show the results of the dynamic analysis of the structure due to the moving load, considering both cases of the initial conditions as explained in the previous section.

Again, we underline that any nodal momentum due to the moving load hasn't been taken into account in this analysis. This might be a non-negligible approximation, but we believe that the results obtained are still meaningful for the purposes of this assignment. Also, any inertia effects due to the acceleration of the load has been neglected. Practically speaking then, the results here presented corresponds to a couple of purely vertical loads applied with different weights over time on the corresponding nodes in order to simulate that the mass is moving along the crane's arm.

As another example of the approximation introduced when considering a subset of mode shapes instead of the whole one, the results here presented are obtained by considering at first just the first 3 mode shapes of the structure and then the first 50 mode shapes.

5.3.1 Initial condition 1

In this case, at the start of the analysis, the structure is found in its undeformed configuration and the load is suddenly added and starts moving at $t = 0$ s.

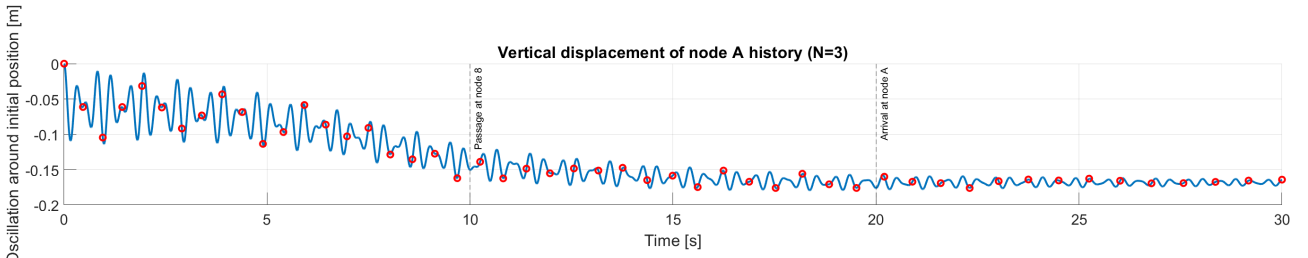


Figure 9: Dynamic response of the structure due to the moving load (initial condition 1, mode shapes considered 3).

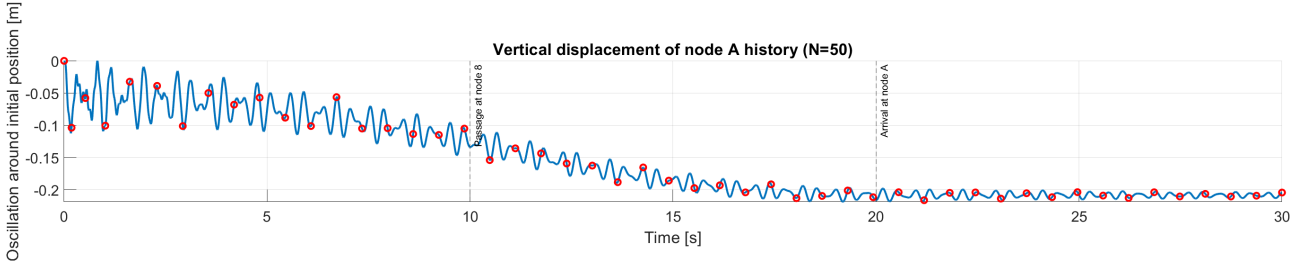


Figure 10: Dynamic response of the structure due to the moving load (initial condition 1, mode shapes considered 50).

As we can see from the time history of node **A**, the structure shows a fast dynamic response due to the sudden addition of the load (in some sense this might be seen as a shock/impact response), overimposed to a slow dynamic response due to the moving load.

5.3.2 Initial condition 2

In this case, the structure starts from its deformed configuration due to the static loads of the mass, which then starts to move along the crane's arm at $t = 0$.

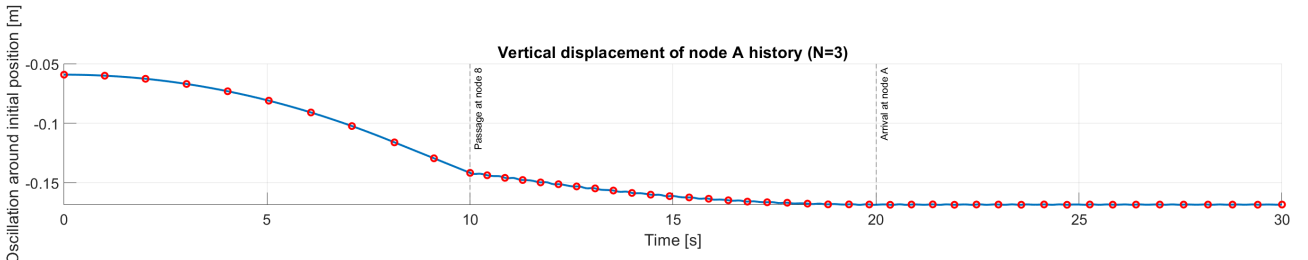


Figure 11: Dynamic response of the structure due to the moving load (initial condition 2, mode shapes considered 3).

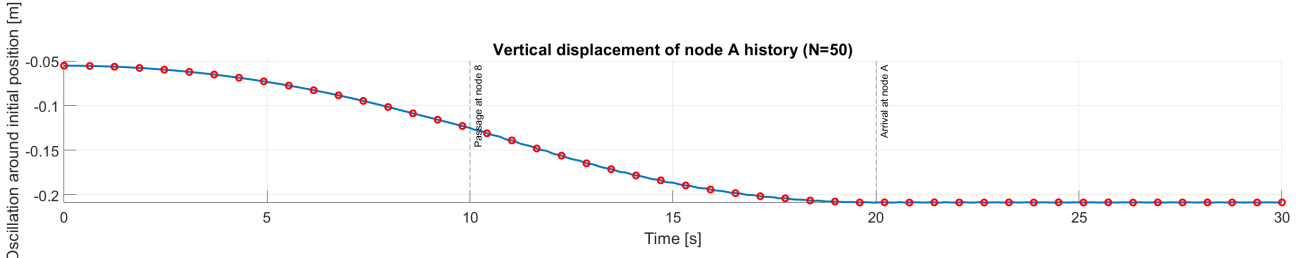


Figure 12: Dynamic response of the structure due to the moving load (initial condition 2, mode shapes considered 50).

As we can see from the time history of node **A**, the structure shows a much more steady and controlled response, with no strong oscillatory behavior. This can be explained by the absence of the equivalent shock/impact response due to the sudden addition of the load.